Journal of Volcanology and Geothermal Research 385 (2019) 143–158

Contents lists available at ScienceDirect

Journal of Volcanology and Geothermal Research

journal homepage: www.elsevier.com/locate/jvolgeores

High-resolution geological investigations to reconstruct the long-term ground movements in the last 15 kyr at Campi Flegrei caldera (southern Italy)

Roberto Isaia[a,*], Stefano Vitale[a,b], Aldo Marturano[a], Giuseppe Aiello[b], Diana Barra[a,b], Sabatino Ciarcia[c], Enrico Iannuzzi[a], Francesco D'Assisi Tramparulo[a]

[a] Istituto Nazionale di Geofisica e Vulcanologia, sezione di Napoli Osservatorio Vesuviano, Via Diocleziano 328, 80124 Napoli, Italy
[b] Dipartimento di Scienze della Terra, dell'Ambiente e delle Risorse (DiSTAR), Università degli Studi di Napoli Federico II, Via Cupa Nuova Cintia 21, 80126 Napoli, Italy
[c] Dipartimento di Scienze e Tecnologie, Università degli Studi del Sannio, Via Francesco De Sanctis snc, 82100 Benevento, Italy

ARTICLE INFO

Article history:
Received 10 November 2017
Received in revised form 8 July 2019
Accepted 13 July 2019
Available online 17 July 2019

Keywords:
Ground deformation
Campi Flegrei
Paleoenvironment
Unrest
Coastal marine sediments
Volcanism

ABSTRACT

Ground deformations are among the main volcanic phenomena occurring within the caldera system and presently recorded at different volcanoes worldwide including the Campi Flegrei active caldera (southern Italy). A new stratigraphic, sedimentological and paleontological survey carried out in the central sector of the Campi Flegrei caldera both along the already known La Starza succession and through a new excavated tunnel provided new insights into the ground movement episodes occurred in the last 15 kyr. This study, which has also benefited of unpublished boreholes stratigraphic data, shows that the most uplifted sector of the Campi Flegrei caldera, presently marked by the morphological structure of the La Starza cliff close to the Pozzuoli coastline, was characterized by a complex sedimentary evolution. It results from different phases of alternating marine transgressions and regressions, the latter marked by both continental volcanic and/or palustrine/lacustrine sediments. These alternations result from the interplay between (i) subsidence and uplift episodes of the caldera floor and (ii) sea level variations during the Holocene. A rest period of volcanism accompanied by a sea level rise determined a significant submersion phase in about 3000 years between 8.59 and 5.5 ka. This phase was defined by a sea level with a maximum water depth value of 60–80 m and a late stage recording significant episodes of ground movements. Subsequently, between 5.5 and 3.5 ka, a ground uplift of about 100 m occurred, with short subsidence around 4.5 ka following the Plinian Agnano-Monte Spina eruption. The net vertical displacement represents the recorded deformation linked with a volcanism period in which 2.5 km^3 of magma were erupted by different vents within the caldera. It is worth to note as the general trend of ground movement through the time indicates a similarity in the pattern, beyond its scale.

1. Introduction

Active caldera volcanic systems are generally characterized by uplift and subsidence phenomena resulting from alternating magma/hydrothermal fluid inflation and deflation processes (e.g., Macedonio et al., 2014; Kennedy et al., 2012). The ground movements can be coupled with volcanism, preceding and following the eruptions, as well as they can occur during periods of volcanic quiescence. In the last decades, spatial and temporal measurements of the ground deformation have been gathered through several geophysical surveys, including Satellite Remote Sensing (e.g., Tizzani et al., 2009; Amoruso et al., 2014). Campi Flegrei (CF; Fig. 1) recently recorded a resurgence caldera process affecting a large urbanized area, which makes it one of the most monitored volcanoes of the world (e.g., D'Auria et al., 2011; Chiodini et al., 2016). Historically, ground movements (bradyseism) on the order of 1–10 m have been detected since Roman times (more than 2000 years ago; e.g., Parascandola, 1947). The Monte Nuovo volcano represents the only example showing important ground uplift (up to 15 m) coupled with an eruptive activity (1538 CE; Guidoboni and Ciuccarelli, 2011; Di Vito et al., 2016). Several models that account for the recent and historical bradyseismic episodes have been proposed by different authors (e.g., Woo and Kilburn, 2010; D'Auria et al., 2015). Information on ground deformation phenomena within the

* Corresponding author.
E-mail address: roberto.isaia@ingv.it (R. Isaia).

https://doi.org/10.1016/j.jvolgeores.2019.07.012

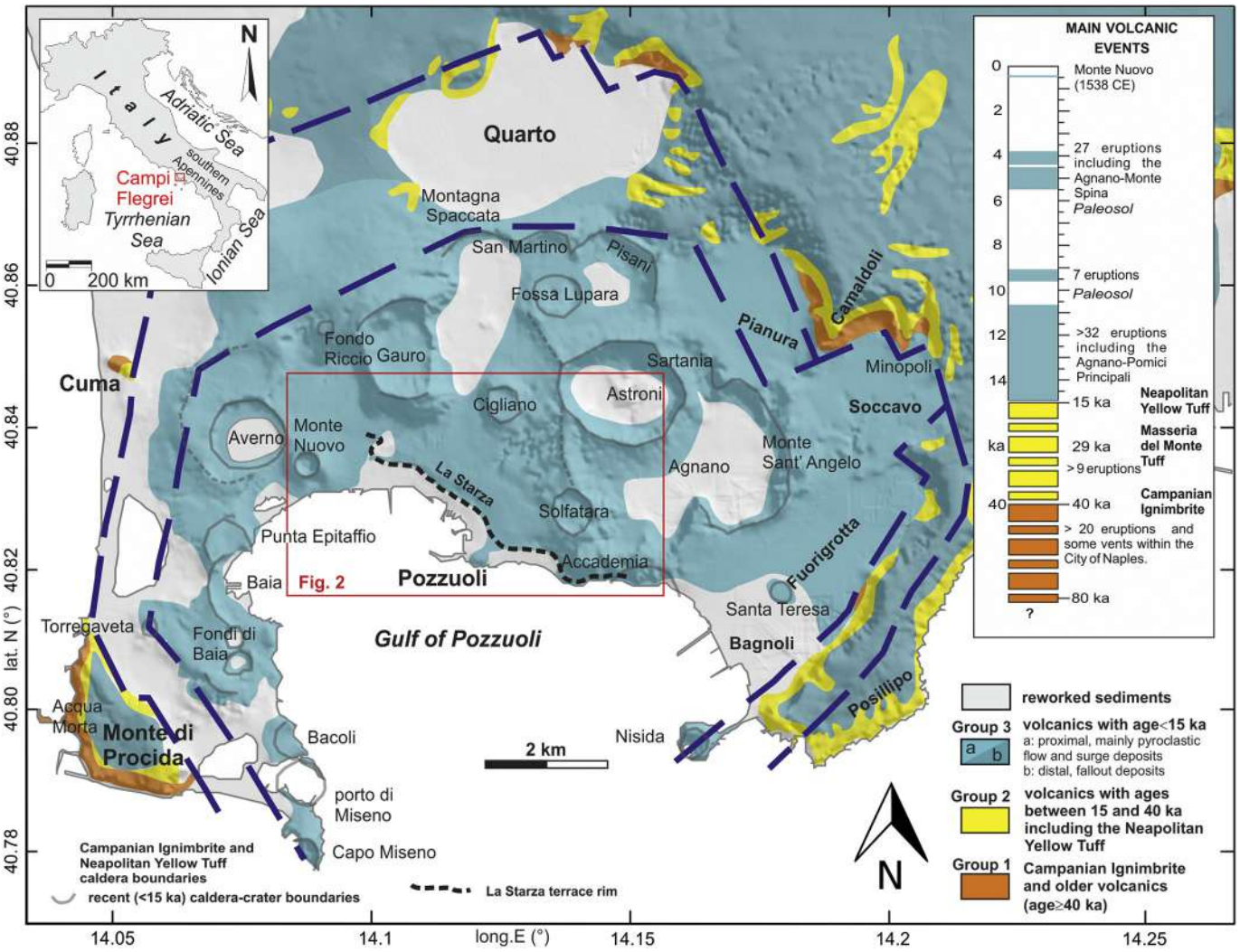

Fig. 1. Simplified geological map of Campi Flegrei (modified after Vitale and Isaia, 2014) and chronologic scheme of the main volcanic events.

caldera have been obtained through a geological study on the marine sequence (e.g., Cinque et al., 1985; Giudicepietro, 1993) presently well exposed along the La Starza cliff (Fig. 2). In particular, the completeness of La Starza succession is fundamental to compare the volcano-tectonic events reconstructed in this sector of the caldera, presently suffering the most intense deformation episode, with those recorded in the whole caldera. The reconstruction of the long-term caldera ground movements, back to the last episode of caldera collapse at about 15 ka, is central to understand the volcano-tectonic processes that accompany volcanism and quiescence of the volcano. Nevertheless, this information can strongly help to define the caldera dynamics through time and can represent a key to interpret the mechanism/process lead to the recent and ongoing ground movements within the CF caldera (e.g., Marturano et al., 2018).

Aim of the present paper is to enhance the knowledge about the stratigraphy, sedimentology, and paleoecology of the sedimentary record of the central caldera sector through investigations of (i) different outcrops exposed along the La Starza, (ii) several successions analyzed during the excavation of a new tunnel joining the area at the foot of the Gauro volcano and the Pozzuoli harbor (Fig. 2), and (iii) new borehole data. The obtained results, combined with the recognition of well-dated CF tephra layers, helped us to estimate the amount of uplift and subsidence occurred in the central sector of the CF from the last episode of caldera collapse (15 ka) to Roman times. Stratigraphy and paleoenvironmental reconstruction of the La Starza cliff was the study subject for different authors (Cinque et al., 1985; Rosi and Sbrana, 1987; Amore et al., 1988; Giudicepietro, 1993; Di Vito et al., 1999; Isaia et al., 2009). However, the tunnel excavation data allowed us to reconstruct the stratigraphic framework better and deposit facies variations, which in turn become of fundamental importance for a more detailed stratigraphy and sampling of the logged marine and transitional sediments. The obtained results allowed us to improve the paleoenvironment interpretation and more precise estimation of the paleobathymetry. As concerns the fossil content analysis and paleoecological interpretations, this paper furnishes a better resolution resulting from a sediment sampling. The comparison of fossil remains, considering especially benthic foraminifer and ostracod assemblages, with the stratigraphic and sedimentological features of the succession allowed the identification of some shallowing and deepening events previously unrecorded.

2. Material and methods

A geological survey, carried out on the La Starza cliff and along an excavation tunnel, allowed us to define the main geological features of the western sector of the central area of the CF caldera. Grain size and paleontological analyses were performed, and information from some well logs has been used to constrain further the reconstruction and evolution of the volcano-tectonic events that occurred in the area. We analyzed and sampled six stratigraphic

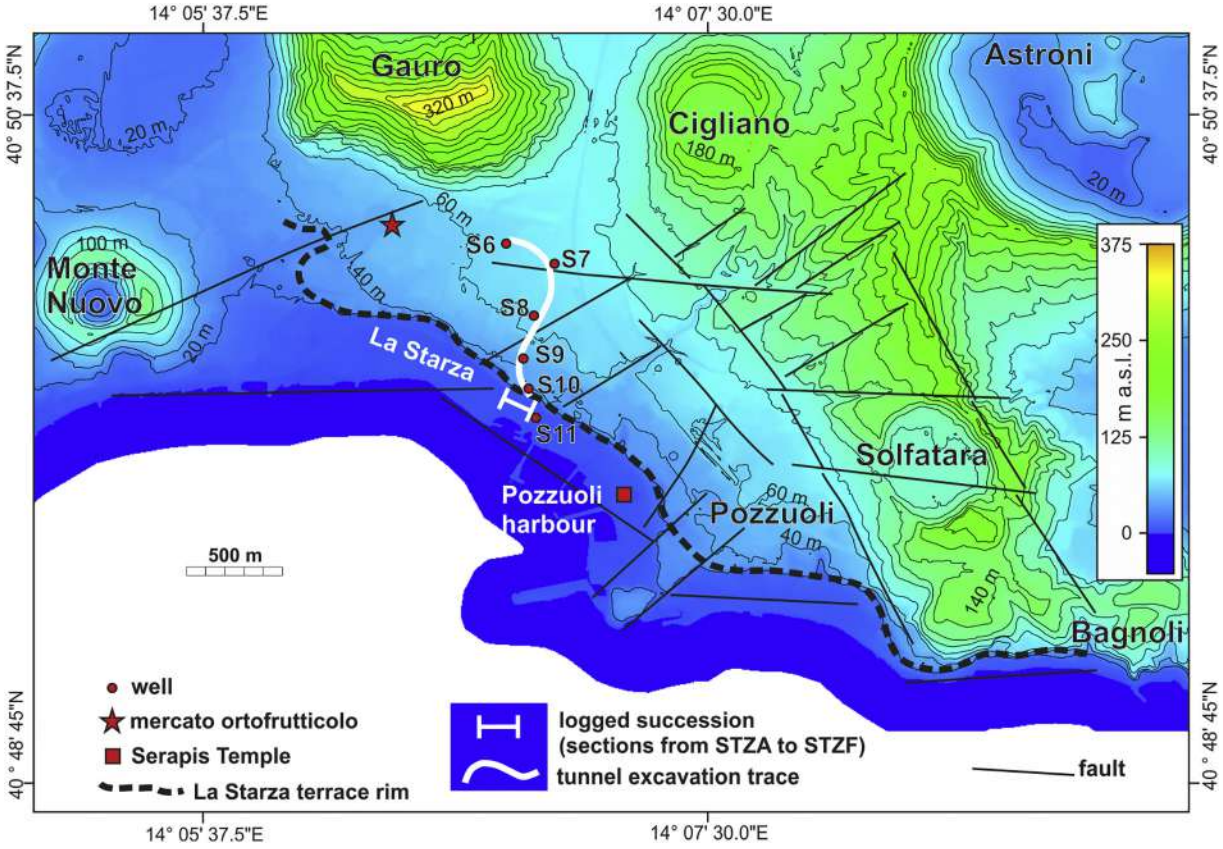

Fig. 2. Topographic map showing the tunnel excavation trace, the location of the geognostic wells and the logged succession along the La Starza terrace rim.

sections (STZA-STZF) along the cliff (Fig. 2) and several tunnel excavation fronts (stratigraphic section TUN). The tunnel starts close to the Gauro volcano and gradually deepens toward south joining the base of the La Starza cliff (5–6 m a.s.l.), after more than 1 km (Fig. 2).

Further information about the stratigraphy of the study area was provided from six prospecting boreholes carried out for the tunnel excavation (S6-S11; Fig. 2), ranging between 20 and 60 m in depth. We performed the grain size analysis on 45 samples collected both within the successions exposed in the tunnel excavation and the La Starza cliff using the classification of Blair and McPherson (1999) to define the grain size classes. By means of the sieve method, the cumulative curves of the percent of passing sediments were calculated and from which we estimated the effective size (D10) and the sorting coefficient S0 defined as $(D75/D25)^{1/2}$, where D10, D25, and D75 are the grain sizes corresponding to the 10–25–75% of passing sediments, respectively.

Paleoecological investigation was carried out on the basis of species identification following the literature on Mediterranean Recent benthic foraminifers (Sen Gupta et al., 2009; Debenay, 2012; Milker and Schmiedl, 2012) and ostracods (Müller, 1894; Barbeito-Gonzalez, 1971; Bonaduce et al., 1976; Breman, 1976; Aiello and Barra, 2010) and their distribution in Recent and Upper Quaternary environments (Aiello et al., 2012; D'Amico et al., 2013; Balassone et al., 2016; Mangoni et al., 2016; Aiello et al., 2018).

The fossil content analysis was performed on 107 samples, of which 54 were fossiliferous containing diatoms, radiolarians, siliceous sponge spicules, serpulid tubes, bivalve, bryozoans, and gastropod remains (mainly tiny fragments), echinoderm spines, planktonic and benthic foraminifers and ostracods (Tables S1, S2 in the Supplementary material). Fossil assemblages are autochthonous or mixed (i.e., including both autochthonous and allochthonous specimens). Only autochthonous fossil remains were considered for the paleoenvironmental analysis.

3. Campi Flegrei volcano

The CF caldera is located along the Tyrrhenian Sea side of the orogenic chain of the southern Apennines in southern Italy (Fig. 1; Vitale and Ciarcia, 2018 and reference therein). The history of CF volcanic field started from at least 80 ka and was characterized by three large volcanic events that formed a 12 km sized caldera (Fig. 1). The oldest, named Campanian Ignimbrite and occurred 40 ka (Giaccio et al., 2008; Costa et al., 2012) has been classified as a super eruption; whereas the second (Masseria del Monte Tuff) and third (Neapolitan Yellow Tuff, NYT) large eruptions occurred 29.3 ka (Albert et al., 2019) and 15 ka (Orsi et al., 1992; Scarpati et al., 1993; Deino et al., 2004), respectively. The following eruption activity took place within the collapsed area through very intense volcanic phases alternating between rest periods. Two longer calm intervals separate the last 15 kyr eruptive history in three main epochs ranging between 15–10.6, 9.6–9.2 and 5.5–3.8 ka, respectively (Di Vito et al., 1999; Smith et al., 2011; Isaia et al., 2015). The last eruption, Monte Nuovo tuff cone located in the western sector of Pozzuoli town (Fig. 2) reported as a historical event, occurred in the 1538 CE after a week of ground deformation activity. The largest number of eruptions took place within the eastern sector of the caldera in short time intervals variable from few decades to centuries (Neri et al., 2015; Bevilacqua et al., 2015, 2017). Simultaneous eruptions from different sectors of the caldera also occurred from Solfatara and Averno volcanoes (Pistolesi et al., 2016). Eruptions were distributed inside the caldera, varying in style and magnitude with a magma emitted volume exceeding 1 km^3 during the major event of Pomici Principali (12.3 ka) and Agnano-Monte Spina (4.55 ka). The volume of erupted magmas is variable through the epochs from 4.2 ± 0.7 to 10.5 ± 0.1 to 2.6 ± 0.5 km^3 of magma (DRE) during the Epoch 1, 2 and 3, respectively.

Table 1
Calibrated ages of the volcanic deposits and marine sediments cropping out along La Starza cliff (1) Di Vito et al., 1999; 2) de Vita et al., 1999; 3) Giudicepietro, 1993; 4) Isaia et al., 2009; 5) Passariello et al., 2010; 6) Rosi and Sbrana, 1987; 7) Smith et al., 2011).

Calibrated ages				Published uncalibrated age			Geographic Coordinates	
Volcanic unit	Age range (ka)	Mean (ka)	Reference	Volcanic unit	Age (ka)	Method	Latitude (°)	Longitude (°)
Fossa Lupara	3.978–4.192	4.085	1; 7	Pre Fossa Lupara	3.820 ± 50	^{14}C AMS		
Astroni 7	4.098–4.297	4.197	1; 7	Pre Astroni 3	3.820 ± 50	^{14}C AMS	40.845830	14.165591
Solfatara	4.181–4.386	4.283	4; 7	Solfatara	3.815 ± 55	^{14}C AMS	40.826565	14.166579
Agnano-Monte Spina	4.482–4.625	4.553	2; 7	Agnano-Monte Spina	5.200 ± 900	Ar/Ar SCTF	40.865049	14.158332
Paleoastroni 2	4.712–4.757	4.734	5; 7	Paleastroni 2	4.215 ± 20	^{14}C AMS	40.865049	14.158332
Monte Sant'Angelo	4.832–5.010	4.921	1; 7	Pre Monte St. Angelo	4.340 ± 50	^{14}C AMS	40.865049	14.158332
Cigliano	5.064–5.431	5.247	1; 7	Pre Cigliano	4.160 ± 50	^{14}C AMS	40.865049	14.158332
Marine sediments				**Marine sediments**				
La Starza (ZR-53)	6.186–5.530	5.858	6; this work	La Starza (ZR-53)	5080 ± 180	^{14}C AMS	40.832939	14.110455
La Starza (s5c2c)	8.846–8.328	8.587	3; this work	La Starza (s5c2c)	8060 ± 100	Counting	40.834130	14.108919
La Starza (ZR-54)	11.237–9.680	10.458	6; this work	La Starza (ZR-54)	9300 ± 350	^{14}C AMS	40.832939	14.110455
La Starza (ZR-55)	11.978–10.481	11.229	6; this work	La Starza (ZR-55)	9850 ± 220	^{14}C AMS	40.832939	14.110455
La Starza (s5c1)	12.418–11.310	11.864	3; this work	La Starza (s5c1)	10,590 ± 140	Counting	40.834130	14.108919

The La Starza terrace is the flat area located in the central part of the CF caldera extending from Monte Nuovo-Gauro volcano to the west, and Bagnoli to the east, seaward bounded by a cliff with a maximum high of ca. 40 m reached in the middle, while it reaches few meters in sporadic outcrops in the easternmost part (Fig. 2; Cinque et al., 1985; Rosi and Sbrana, 1987; Giudicepietro, 1993; Orsi et al., 1996). The stratigraphic succession exposed along the sea cliff is made up by prevailing marine sediments alternating to volcanic deposits mainly localized in the uppermost part.

Previous studies on La Starza succession (Cinque et al., 1985; Rosi and Sbrana, 1987; Amore et al., 1988; Giudicepietro, 1993; Orsi et al., 1996; Di Vito et al., 1999; Isaia et al., 2009) indicate that the succession is defined by an alternation of marine and continental deposits of volcanic origin, both younger than the NYT eruption. Most of the authors reported the presence of marine deposits up to a certain height along the cliff, below the volcanic deposits of the most recent activities of CF including the eruptions of Agnano–Monte Spina (AMS) and Astroni. The Plinian AMS eruption (4.55 ka; de Vita et al., 1999; Smith et al., 2011) determined the minor caldera collapse of the Agnano plain (Fig. 1) followed by a general subsidence of the CF caldera and finally some uplift phases (Isaia et al., 2009) associated to the eruptive activity from vents located in the central caldera sector (Isaia et al., 2015). Fossiliferous marine sediments, localized at different stratigraphic heights, were previously dated by radiocarbon method (Rosi and Sbrana, 1987; Giudicepietro, 1993), which resulting ages were calibrated using the INTCAL13 procedure (Reimer et al., 2013) and here presented in Table 1.

4. Results

4.1. Stratigraphy

The exposed lower part of the succession of La Starza cliff (Fig. 3) is composed by 1 m of alternating fine, medium and coarse-grained sands, upward passing to 2.5 m thick of medium-coarse sands (Fig. 4A), locally characterized by cross-lamination (Fig. 4B) and pumice lenses. This deposit is overlain by a 1 m thick level of yellowish/mauvish rhythmically laminated silt and fine sand, hereafter called "marker level#1" (Fig. 4A), in turn, covered by 2 m of fine to coarse sands and pumice lenses, and finally 0.2 m (Fig. 4A) to 3 m (Fig. 4F) of medium-coarse orange- brownish massive sands, hereafter called "marker level#2". In the tunnel excavation, the lowest part of the succession (Fig. 4C) is composed of fine-medium grained sands covered by coarse-grained channelized sands (Fig. 4D, E) alternating with pumice and scoria coarse lenses, in turn covered, through an angular unconformity (Fig. 4C), by fine sediments (Fig. 4F), corresponding to the marker level#1 exposed along the La Starza cliff. In both La Starza cliff and tunnel excavation the succession upward continues with 5 m of medium to fine massive, containing several remnants of fossils as mollusk shells, corals (e.g., *Cladocora caespitosa*; Fig. 4G) and echinids (e.g., *Schizaster*; Fig. 4G). A sharp surface marks a change in the succession passing to three layers ("marker level#3") of fine to medium sands with rounded pumice lenses (Fig. 4A), for a total thickness of ca. 3 m. Each layer includes at the base *Posidonia oceanica* rizholites (mattes), with gastropod and ostreid shells (Fig. 5A, D) and are covered by medium-fine massive sands locally with *P. oceanica* leaves and gastropod shells (Fig. 5B, C), somewhere containing vegetal fragments and plant frustules. In the La Starza cliff, these marine deposits are upward confined by a clearly visible sharp surface likely due to the differential erosion with the overlying coarser pyroclastic deposits (Fig. 4A). On the contrary, in the tunnel excavation, the marine sands abruptly pass upward through an unconformity, to alternating coarse-grained sands and few decimeters horizontal stratified beds containing pumices, scoria and rounded pebbles and cobbles made of lava and tuff (Fig. 5D, E). These beds show a high lateral persistence, and locally host massive sands within large lobe-shaped channels (Fig. 5F) and well-sorted coarse-grained sands, granules and fine-grained pebbles (Fig. 5E). These coarse-grained deposits correspond to similar sediments elsewhere exposed in the Pozzuoli area, such as those described by Cinque et al. (1985) close to the "mercato ortofrutticolo" (Figs. 2 and 5G) and presently hidden by the intense urbanization. Finally, the succession is capped by a sequence mainly composed of volcanic deposits already described by different authors (Cinque et al., 1985; Rosi and Sbrana, 1987; Giudicepietro, 1993; Di Vito et al., 1999; Isaia et al., 2009) along the La Starza cliff. The lower part of the succession contains prevailing coarse ash beds and pumice lenses with cross-lamination to sand-wave structures up grading to plane-parallel massive and fine ash layers with variable thickness and colors. Pyroclastic deposits are separated by erosional unconformities or thin paleosols. A similar succession was excavated at the northern entrance of the tunnel. This stratigraphic setting has also been supported by available calibrated ages presented in Smith et al. (2011). The pyroclastic deposit features, including intercalated erosional unconformities and paleosols, allowed us to correlate them, from the bottom to the top, to the products of Cigliano (5.250 ka), Monte Sant'Angelo (4.920 ka), Paleoastroni 2 (4.730 ka), Agnano Monte-Spina (4.550 ka), Paleoastroni 3, Averno-Solfatara (4.280 ka), Astroni (4.250 ka), Fossa Lupara (4.200 ka) and Monte Nuovo units (1538 CE) (Fig. 6A, B; Table 1), as defined by previous studies in the surroundings area (Di Vito et al., 1999; Isaia et al., 2009).

The volcanic succession, exposed along La Starza cliff, also contains a discontinuous layer, embedded between the pyroclastic flow deposits of Agnano-Monte Spina and the fallout beds of

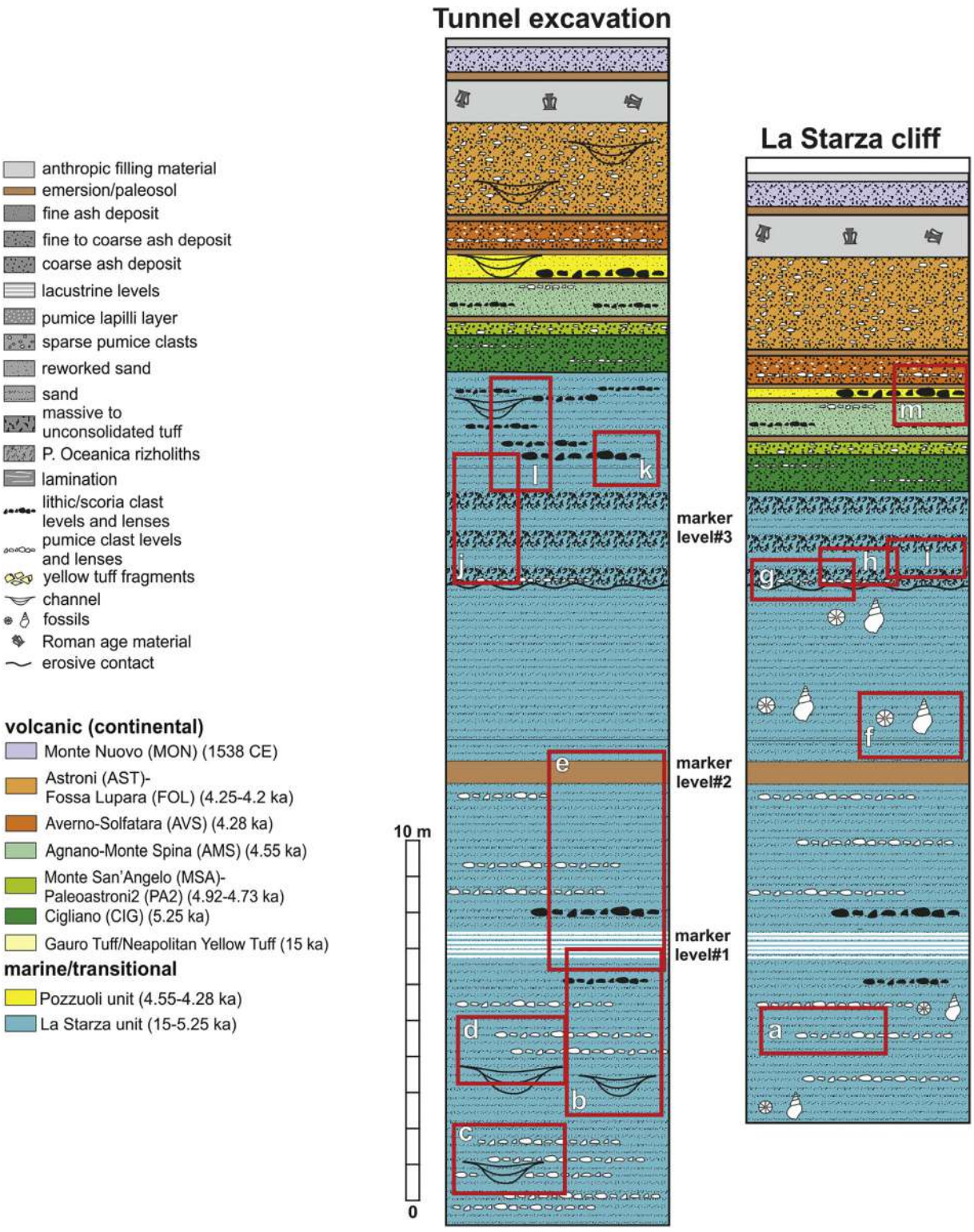

Fig. 3. Schematic stratigraphic logs of tunnel excavation and La Starza outcrop. a–f: Fig. 4B–G; g–m: Fig. 5A–H.

Averno-Solfatara deposits. This layer, with a maximum thickness of 30 cm (Fig. 5H), is composed of a humified dark grey sandy layer containing large rounded pebbles and cobbles of lavas, tuffs, and scoriae. Along the excavation front of the tunnel entrance (Fig. 6A, B) normal faults crosscut the Agnano-Monte Spina deposits in turn sealed by the Averno-Solfatara tephra (Fig. 6A, B). The volcanic succession hosts several channels and structural depressions; the largest is bounded by normal faults and filled by intensely bioturbated, fine volcanic ashes at base (Fig. 6C–E). These sediments are cut by several sand dikes and covered by laminated reworked sands locally with asymmetric ripples (Fig. 6E) interpreted by Vitale et al. (2019) as layers of seismically induced sand volcanoes. It is worth to note that the overlying volcanic layers are again pedogenized with further pervasive bioturbation.

Further stratigraphic information comes from geognostic wells within the area between the Gauro and the Pozzuoli harbor (Fig. 2).

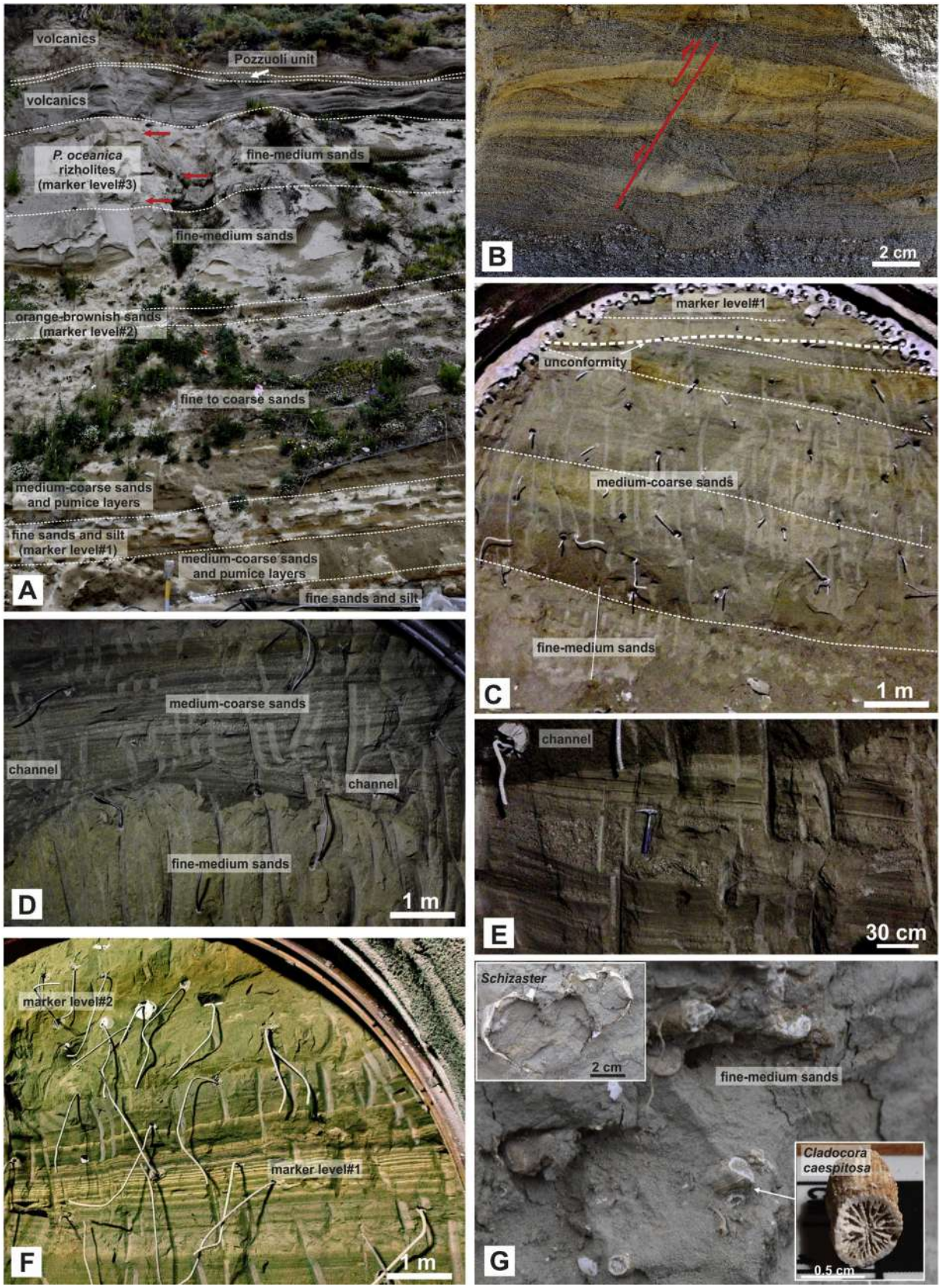

Fig. 4. A) La Starza cliff. B) Cross-lamination in sands. C) Moderately W-dipping sand deposits covered by flat-lying fine sediments. D) Channelized coarse deposits overlying fine-medium sands. E) Channelized deposits in the coarse deposits. F) Central part of the succession showing the two marker levels. G) Fine-medium sands with *Cladocora caespitosa* colony and *Schizaster*.

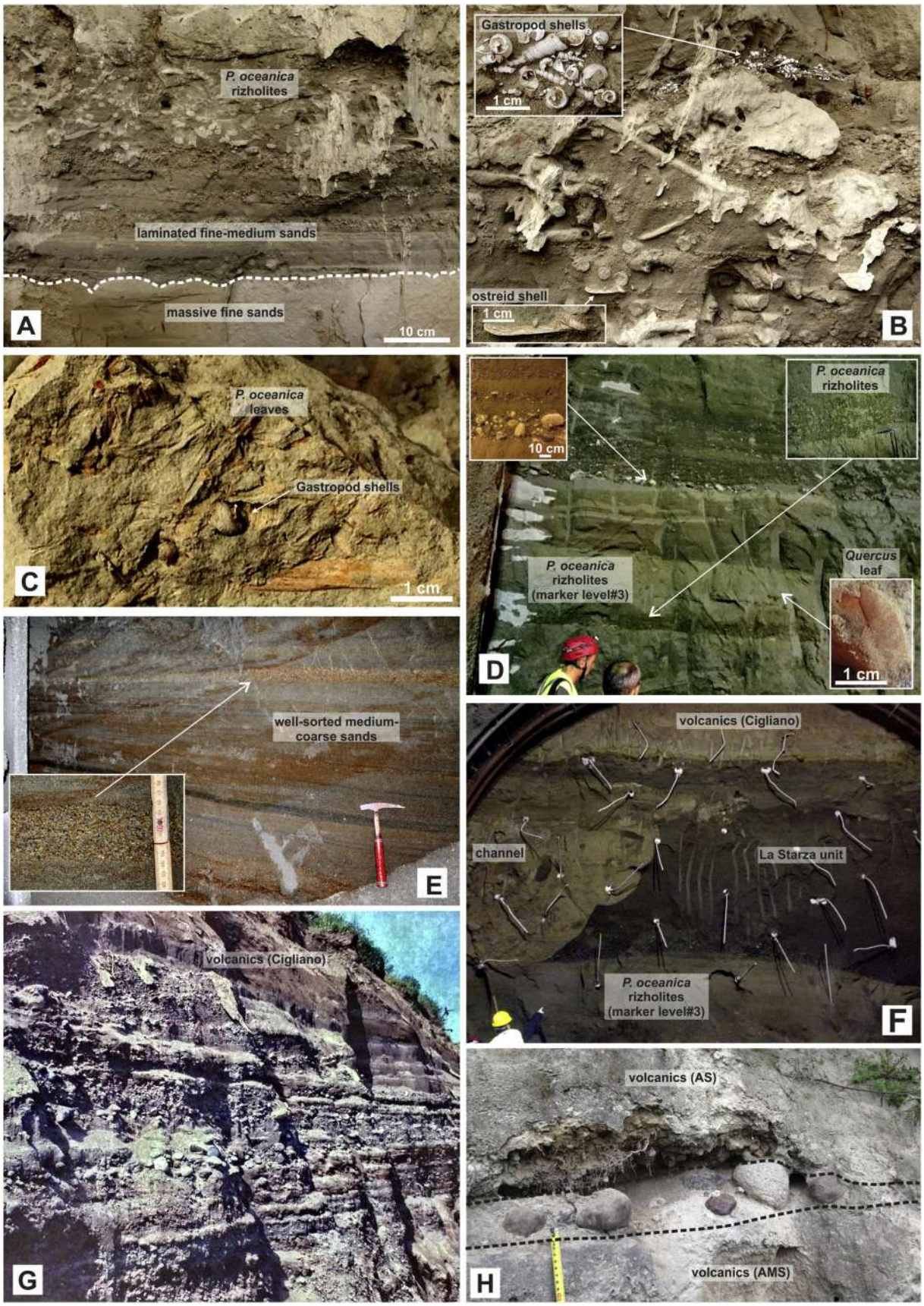

Fig. 5. A) Erosive contact between marine circalittoral sediment (on bottom) and marine infralittoral and *P. oceanica* rizholites (on top) (La Starza cliff). B) Sands with *P. oceanica* rizholites, ostreid and gastropod shells (marker level#3; La Starza cliff). C) Sands with *P. oceanica* leaves and gastropod shells (marker level#3; La Starza cliff). D) Three levels of sands with at base *P. oceanica* rizholites (marker level#3) upward passing to coarse sediments with pebble layers (tunnel excavation). E) Flat-lying levels of well-sorted coarse sands and pebbles (tunnel excavation). F) Upper part of the La Starza unit showing a large channel with lobate shape covered by the volcanic deposit of the Cigliano eruption (tunnel excavation). G) 80's photo of the upper part of the La Starza unit cropping out in the Pozzuoli area ("mercato ortofrutticolo").

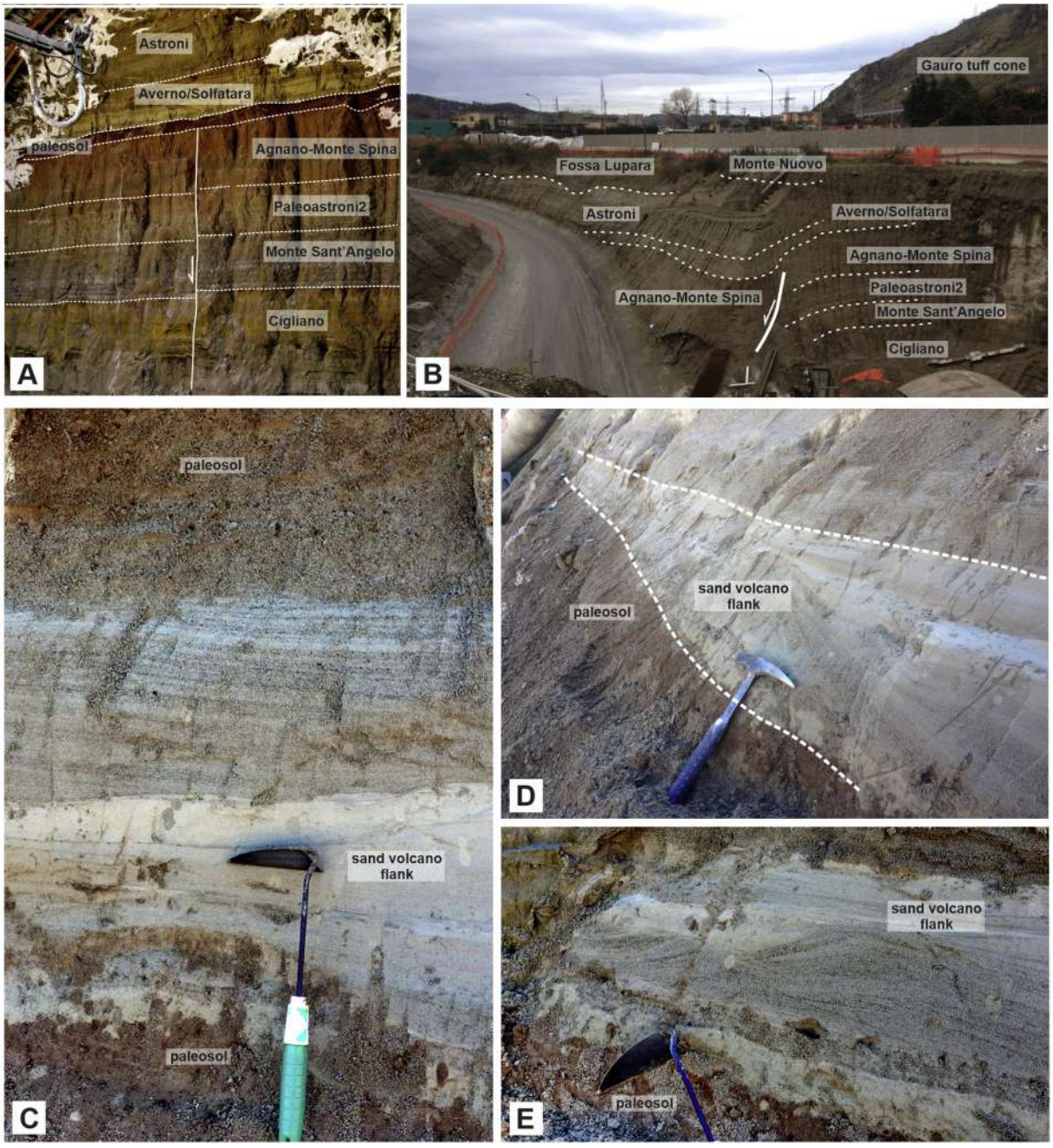

Fig. 6. A) Upper part of the succession manly characterized by volcanic deposits showing an almost vertical normal fault hosted in Cigliano to Agnano-Monte Spina tephra and sealed by the paleosol underlying the Averno-Solfatara volcanic deposits. B) Panoramic view of the tunnel entrance excavation. C–E) The Pozzuoli unit sands.

Wells, from S6 to S10 (Fig. 7), shows an upper part characterized by the above described volcanic sequence, whereas, in the wells S6, S8, and S9, the Agnano-Monte Spina deposits are partially or totally substituted by the sediments of Pozzuoli unit formed by reworked volcanic sands. Below the volcanic sequence and the Pozzuoli unit, La Starza sediments have been recognized. Only in the well S9 the La Starza sediments lie on the Gauro tuff (14.3 ± 0.9 ka; Di Renzo et al., 2011), which were erupted soon after or simultaneously to the NYT eruption generating a ca. 40 m thick deposit. The well S11 is located at the foot of the La Starza cliff below reworked Roman sediments at a lower elevation (ca. 6 m a.s.l.) and is entirely characterized, for a thickness of ca. 20 m, by fine to coarse sands of the basal part of the La Starza succession (for a complete description see Table S3 in the Supplementary material). The grain size analysis shows as the curve of the effective size (Fig. 8A) is dominantly medium sands, with the finest sediments located between 17 and 18 m from the base of the measured section (Fig. 8A). The sorting coefficient curve (Fig. 8B) indicates dominant well-sorted and uniform sands with some poorly sorted sands, especially above the channelized and erosional surfaces.

4.2. Micropaleontological content

In the following section, the data of micropaleontological assemblages are presented from the tunnel section (TUN) to the 6 sections exposed in the La Starza cliff (from STZA to STZF; Table 2; Fig. 9; Aiello et al., 2018). In the Tunnel section, most of the samples (TUN 1, 3–21, 24–26, 28–34, 36–38) was barren. The remaining five samples yielded assemblages dominated by siliceous remains. TUN 2, 22, 27 and 35 consisted almost exclusively of sponge spicules; TUN

Table 2
Synthesis of fossil contents and relative paleoenvironmental reconstruction. Infralittoral: the region of shallow water closest to the shore (from the low tide level down to -30/-40 m). Circalittoral: the region extending from the lower limit of the infralittoral down to the maximum depth at which photosynthesis is still possible (-100/-200 m).

n	STZA samples
STZA 8-13	Devoid of fossil remains.
STZA 1-7	Siliceous microfossil remains (diatoms, radiolarians and sponge spicules) largely dominate the assemblagesPaleoenvironment: low pH marine waters; paleodepth changes not detectable
n	**STZB samples**
STZB 7-10	Siliceous microfossil remains (radiolarians and sponge spicules) largely dominate the assemblagesPaleoenvironment: low pH marine waters; paleodepth changes not detectable
STZB 5-6	Siliceous and calcareous remains are present, including diatoms, sponge spicules, echinoderm spines, middle abundance, and diversity foraminifer assemblages and low abundance and diversity ostracod assemblages. The foraminifer species *Elphidium granosum*, *Nonionella turgida,* and *Reussella spinulosa* and the ostracods *Costa edwardsi* and *Semicytherura incongruens* dominate the assemblagesPaleoenvironment: marine waters, possibly upper circalittoral zone
STZB 2-4	Only siliceous fossil remains (rare and minute sponge spicules)Paleoenvironment: low pH marine waters; paleodepth changes not detectable
STZB 1	Devoid of fossil remains
n	**STZC samples**
STZC 35	Only siliceous spicules are recordedPaleoenvironment: low pH marine waters; paleodepth changes not detectable
STZC 27-34	Siliceous and calcareous microfossil remains, including sponge spicules, diatoms, foraminifers, ostracods, and echinoderm spines; This interval yielded the most diversified assemblages. The foraminifer species richness ranges from 31 to 48, that of the ostracods from 19 to 28. In comparison with the underlying sub-interval, Rotaliidae and Elphidiidae, as well as the subordinate species *R. spinulosa* and *Bulimina elongata* show a decrease; percentages of *Asterigerinata adriatica*, *Buccella granulata*, *Bolivina lowmani*, *Gavelinopsis praegeri,* and *Rectuvigerina phlegeri* are generally higher. Rare miliolids occur. The ostracod assemblages are characterized by high frequencies of *Costa edwardsi*, *Carinocythereis whitei,* and *Cistacythereis* (*H.*) *turbida*. *Semicytherura* spp. and *Rectobuntonia subulata* increase. *Pseudopsammocythere reniformis* and *Leptocythere ramosa* continue to be well representedPaleoenvironment: upper circalittoral, from slightly stressed to normal marine waters. Maximum paleodepth probably around 60/80 m bsl
STZC 19-26	Siliceous and calcareous microfossil remains, including sponge spicules, foraminifers, ostracods and echinoderm spines; middle-low abundance and diversity foraminifer and ostracod assemblages. Benthic foraminifers dominated by Elphidiidae, *N. turgida*, Rotaliidae, and, subordinately, by *A. adriatica*, *B. elongata*, *G. praegeri*, *Haynesina depressula,* and *R. spinulosa*. Ostracod assemblages are characterized by high percentages of *C. edwardsi*, *C. whitei*, *C.* (*H.*) *turbida*, *Xestoleberis dispar*, *P. reniformis* and *L. ramosa*Paleoenvironment: upper circalittoral, slightly stressed marine waters. A further deepening and a relative amelioration of bottom water conditions occur
STZC 17-18	Calcareous microfossil remains, including foraminifers and ostracods and echinoderm spines; ostracod assemblages with low abundance and diversity. The foraminifer genera *Ammonia* and *Elphidium* dominate the assemblage of sample STZC 17. In the sample STZC 18 high foraminifer Species richness, the first occurrence of the ostracod *C. edwardsi*, and the presence of siliceous remains have been recorded. *N. turgida* and *B. elongata* are the most represented foraminifer speciesPaleoenvironment: slightly undersaturated in calcium carbonate, low oxygen, marine waters. A transgressive trend from infralittoral zone to lower infralittoral - upper circalittoral zone occurs
STZC 15-16	Siliceous and calcareous microfossil remains, including foraminifers, ostracods and echinoderm spines; first occurence of ostracods. Assemblage of sample STZC 15 is characterized by high abundance of *A. adriatica* and *N. turgida* (foraminifers) and *Cytheridea neapolitana* (ostracod). The foraminifer genera *Ammonia* and *Elphidium* dominate the assemblage of sample STZC 16Paleoenvironment: marine waters, probably in lower infralittoral/upper circalittoral zone, slightly undersaturated in calcium carbonate. A shallowing trend is recognized, culminating in a brief emersion phase represented by a pedogenized level ranging from 20.2 to 20.9 m asl
STZC 7-14	Barren sediments alternate fossiliferous layers; assemblages very poor, including rare sponge spicules (STZC 7, STZC 9, STZC 13), radiolarians (STZC 9) and foraminifers (STZC 7, STZC 13); ostracods not presentPaleoenvironment: marine waters with unfavorable varying physico-chemical conditions
STZC 1-6	Devoid of fossil remains
n	**STZD samples**
STZD 1-2	Devoid of fossil remains
n	**STZE samples**
STZE 3-5	Siliceous microfossil remains, including sponge spicules, largely dominate the assemblages, very rare mollusk fragments occurPaleoenvironment: low pH marine waters; paleodepth changes not detectable
STZE 2	Siliceous and calcareous remains are present, including foraminifers, sponge spicules, echinoderm spines; middle abundance and diversity foraminifer assemblages and low abundance and diversity ostracod assemblage. The foraminifer species *E. granosum*, *N. turgida, Elphidium poeyanum* DS form, *Ammonia aberdoveyensis* lobate form dominate the assemblage; ostracods not presentPaleoenvironment: marine waters, possibly lower infralittoral - upper circalittoral zone
STZE 1	Siliceous and calcareous remains are present, including foraminifers, sponge spicules, bryozoan, and mollusk remains, echinoderm spines; middle abundance and diversity foraminifer assemblages and low abundance and diversity ostracod assemblage. The foraminifer species *E. granosum*, *E. crispum, E. poeyanum* DS form, *A. aberdoveyensis* lobate form and the ostracods *C. edwardsi* and *S. incongruens* dominate the assemblagePaleoenvironment: marine waters, possibly lower infralittoral - upper circalittoral zone
n	**STZF samples**
STZF 4	Siliceous and calcareous microfossil remains, including sponge spicules, foraminifers and echinoderm spines; middle abundance and diversity foraminifer. Benthic foraminifers dominated by *N. turgida*, *A. aberdoveyensis* lobate form, *E. crispum,* and *R. phlegeri*; ostracods rarePaleoenvironment: marine waters, probably in lower infralittoral - upper circalittoral zone, slightly undersaturated in calcium carbonate
STZF 2-3	Siliceous and calcareous microfossil remains, including sponge spicules and echinoderm spines; low abundance and diversity foraminifer. Benthic foraminifers dominated by *B. granulata*, *Ammonia aberdoveyensis* rounded form, *E. crispum*; ostracods not presentPaleoenvironment: marine waters, probably in lower infralittoral - upper circalittoral zone, slightly undersaturated in calcium carbonate
STZF 1	Siliceous and calcareous microfossil remains, including sponge spicules, foraminifers, and echinoderm spines; middle abundance and diversity foraminifer. Benthic foraminifers dominated by *N. turgida*, *E. crispum*, , *A. aberdoveyensis* lobate form, *E. poeyanum* DS form; ostracods not presentPaleoenvironment: marine waters, probably in lower infralittoral - upper circalittoral zone, slightly undersaturated in calcium carbonate
n	**TUN samples**
TUN 36-38	Devoid of fossil remains
TUN 35	The samples yielded mostly siliceous fossil remains (uncommon sponge spicules). Paleoenvironment: low pH marine waters; paleodepth changes not detectable
TUN 28-34	Devoid of fossil remains
TUN 27	The samples yielded mostly siliceous fossil remains (uncommon sponge spicules). Paleoenvironment: low pH marine waters; paleodepth changes not detectable
TUN 24-26	Devoid of fossil remains
TUN 23	The samples yielded mostly siliceous fossil remains (rare sponge spicules and diatoms). Paleoenvironment: low pH marine waters; paleodepth changes not detectable
TUN 22	The samples yielded mostly siliceous fossil remains (common sponge spicules). Paleoenvironment: low pH marine waters; paleodepth changes not detectable
TUN 3-21	Devoid of fossil remains
TUN 2	The samples yielded mostly siliceous fossil remains (rare and minute sponge spicules). Paleoenvironment: low pH marine waters; paleodepth changes not detectable
TUN 1	Devoid of fossil remains

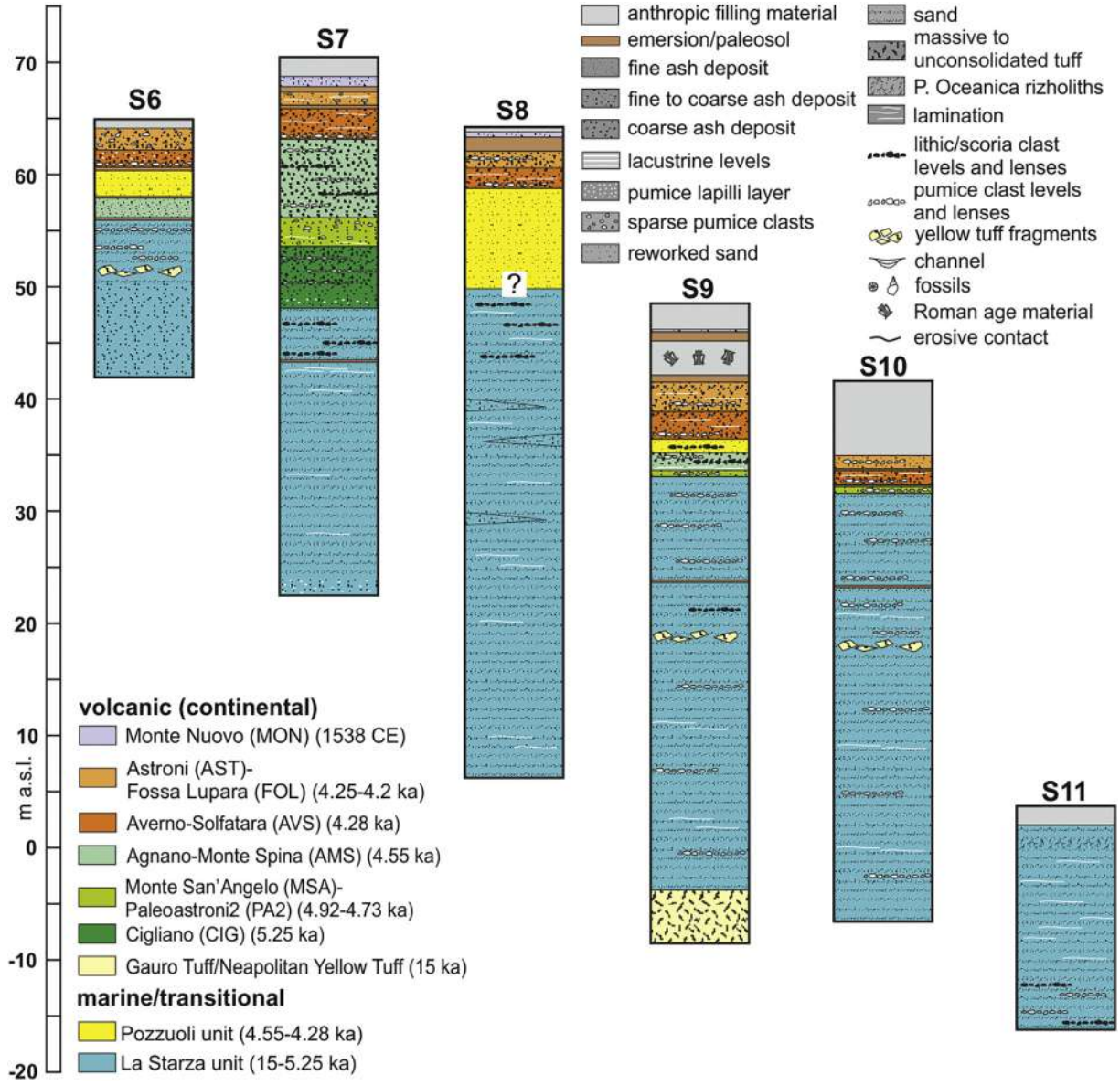

Fig. 7. Interpreted logs (see Fig. 2 for the good localization).

23 also contained large diatoms. Along the STZA section, siliceous remains (diatoms, sponge spicules, and radiolarians) dominate largely the assemblages (samples STZA 1–7), whereas the sediments of the upper part of the section (STZA 8–13) are barren. In the STZB section, the sample STZB 1 is devoid of fossil remains, whereas in the samples STZB 2–4 minute siliceous sponge spicules occur. Samples STZB 5 and STZB 6 yielded siliceous and calcareous remains, including foraminifers, ostracods, diatoms, radiolarians, sponge spicules, and echinoderm spines. Benthic foraminiferal assemblages show middle abundance and diversity values; ostracod assemblages are characterized by high dominance and low diversity/abundance values. The assemblages of the uppermost part of the section (sample STZB 7–10) consist almost exclusively of siliceous remains (sponge spicules and radiolarians). The STZC section show, in the lower part, microfossil assemblages are not present (samples STZC 1–6). The overlying interval displays an alternation of fossiliferous and barren layers (STZC 7–14). The samples STZC 8, STZC 10–12, STZC 14 are devoid of fossil remains. In the remaining samples, the assemblages are generally poor and consist of rare sponge spicules associated with radiolarians (STZC 9) or benthic foraminifers (STZC 7, STZC 13). In the sample STZC 7 foraminifers are represented by a single specimen of *Elphidium granosum*; the assemblage recorded in the sample STZC 13 consists of 19 species, the most abundant being *Ammonia aberdoveyensis, Ammonia falsobeccarii*, *Elphidium poeyanum*, and *Buccella granulata*. Ostracod shells have not been recorded in this interval. In the upper part of the section, that includes all the samples (STZC 15–34) showing the co-occurrence of benthic foraminiferal and ostracod assemblages, abundance and diversity are relatively high. The samples STZC 18–34 were the most reliable for paleoecological interpretation. In all the samples are present echinoderm spines; in the main part of the samples, sponge spicules, planktonic foraminifers, mollusks, radiolarians, diatoms, and serpulids are associated in decreasing order of frequency. The uppermost sample of the section STZC (STZC 35) yielded exclusively common sponge spicules. In the STZD section, the two layers sampled (STZD 1–2) resulted devoid of microfossil remains. Along the STZE section, the lowermost sample (STZE 1) yielded siliceous, and calcareous remains, including foraminifers, ostracods, sponge spicules, bryozoan, and mollusk remains, and echinoderm spines. We observed

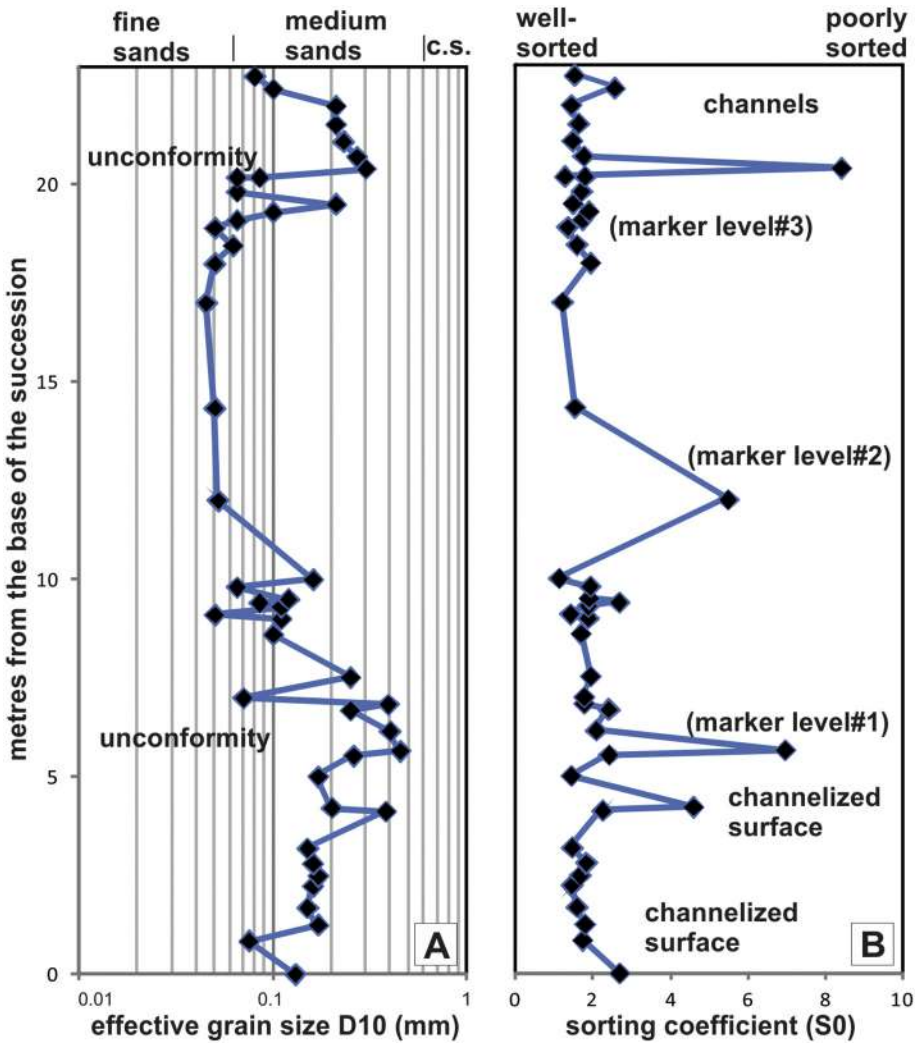

Fig. 8. Profiles across the La Starza unit: A) effective size and B) sorting coefficient. f.s.: fine sand; m.s.: medium sand; c.s.: coarse sand.

middle and low values of foraminiferal and ostracod assemblage abundance and diversity, respectively. The foraminiferal species *Elphidium granosum*, *E. crispum*, *E. excavatum*, *A. aberdoveyensis*, and the ostracods *Costa edwardsii* and *Semicytherura incongruens* dominate the assemblage. In the sample STZE 2 foraminifers, sponge spicules, echinoderm spines occur. The foraminiferal assemblage is dominated by *E. granosum*, *Nonionella turgida*, *E. poeyanum*, *A. aberdoveyensis*. Ostracods are not present. Assemblages of the samples STZE 3–5 consist mostly of siliceous sponge spicules. Neither ostracod nor foraminiferal remains occur. In the STZF section, the sample STZF 1, collected at the base of the section, yielded siliceous and calcareous microfossil remains, with sponge spicules, foraminifers, and echinoderm spines. Foraminiferal assemblage is dominated by *N. turgida*, *E. crispum*, *A. aberdoveyensis*, and *E. poeyanum*. Ostracods are not present. Siliceous sponge spicules and echinoderm spines are present whereas ostracods lack. The uppermost sample (STZF 4) of section F yielded both benthic foraminiferal and ostracod assemblages.

5. Discussion

The paleoenvironmental reconstruction (Fig. 9B) has been obtained joining paleoecological and sedimentary facies descriptions. The presented stratigraphy, combined with the available age determinations (Table 1; Fig. 9D), allowed us to highlight the timing of the variation of the depositional environments from marine to continental as a result of the relative movement between the sea level and the ground deformation of the caldera. Seven main stratigraphic intervals have been defined (a–g) corresponding to different paleoenvironments (Fig. 9B) and bathymetric zonations (Fig. 9C) before the emersion of La Starza and the deposition of the pyroclastic rocks of the Epoch III (interval h; Fig. 9B). The succession starts with sediments deposited in a backshore transitional environment (interval a; Schwartz, 1982; Barra et al., 1998) evolving upward to deposits formed in a foreshore/shoreface environment and related to an upper infralittoral zone, at least in part, in low pH marginal waters (interval b; Clifton, 1981; McCubbin, 1982; Hart and Plint, 1995). These deposits immediately overly the sediments collected in the same area and dated at about 12 ka (Fig. 9D, Table 1; Giudicepietro, 1993). The succession continues upward with sediments locally containing fossils related to marine waters with unfavorable varying physicochemical conditions and showing sedimentary structures related to coastal lacustrine/foreshore conditions, like a paralic setting, from marginal to upper infralittoral zone (interval c; Carobene and Brambati, 1975; Ciarcia and Vitale, 2013, and references therein). The lower part is characterized by the fine varved lacustrine layers named as marker level#1 (Fig. 4A, C, F), which has been recognized for many hundreds of meters also in the tunnel excavation. It could correspond to the rest stage between the Epoch I and II (Fig. 9A, B). The over-

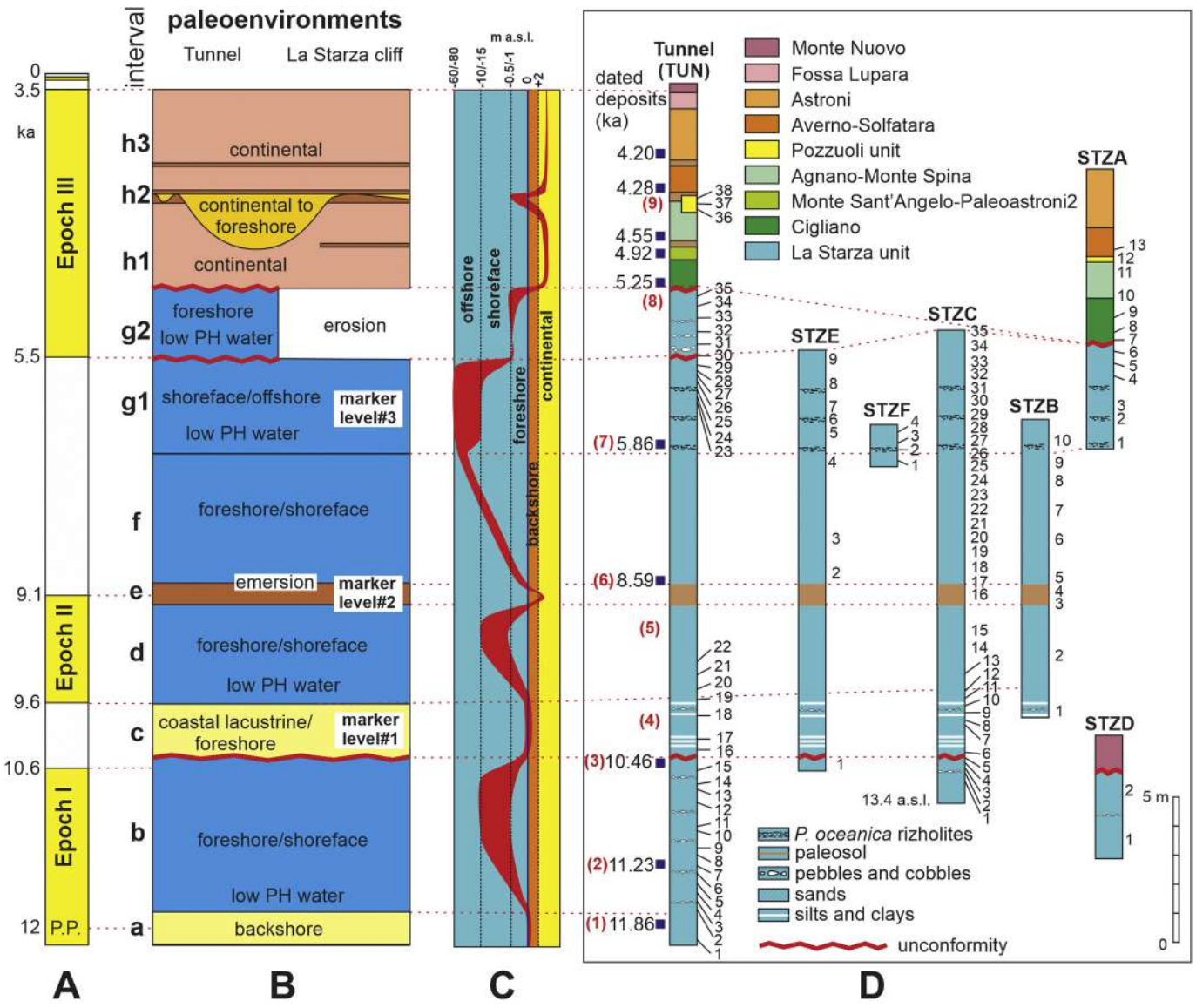

Fig. 9. A) Volcanic epochs. P.P.: Pomici Principali eruption. B) Reconstructed paleoenvironments. C) Paleobathymetric profile. D) Seven sections with sampling location and dated deposits.

lying deposits show fossil assemblages indicating bottom water stress conditions in a foreshore/shoreface environment, from upper infralittoral to marginal zone (interval d), which precedes an emersion phase (interval e) marked by the orange-brown coarse sandy pedogenised layer (level marker#2). The emersion of La Starza succession likely occurred before a transgressive phase started about 8.59 ka (Fig. 9D; Table 1), according to Giudicepietro (1993), marked by fossil assemblages of the infralittoral zone, in slightly undersaturated calcium carbonate waters. A relative amelioration trend of the bottom water environmental conditions, as well as a deepening toward an upper circalittoral zone, was progressively recorded upward (foreshore/shoreface environments; interval f). The overlying interval is characterized by three similar deposits containing *P. oceanica* rizholites and fossil assemblages, indicating a lower infralittoral zone alternating with fine sediments with circalittoral microfossils (marker level#3). This succession suggests abrupt variations of the paleodepth from infralittoral to circalittoral zone and from shoreface to offshore sedimentary environment (interval g1; e.g., Swift et al., 2009). The uppermost gravelly and sandy layers occurrence suggest a variable continental to the shallow-water marine environment (foreshore), with a large amount of reworked volcanic material (interval g2; e.g., Massari and Parea, 1988). Deposit at the base of stage g was dated about 5.86 ka (Fig. 9D; Table 1; Rosi and Sbrana, 1987) and could be the surficial response to the deep magma injection preceding the eruptions of Epoch III (from about 5.5 ka). This phase was characterized by at least four cycles of abrupt uplifts and subsequent subsidences, with the last cycle (interval g2; Fig. 9B) likely synchronous with the small volume volcanism predating the first eruptions of the III epoch occurred few km far from la Starza (Agnano1-2 and Averno1 eruptions; Smith et al., 2011; Table 1). Between the La Starza unit and the overlying Cigliano deposit, an erosional surface, was formed. This erosion was probably related to the emersion of the La Starza succession occurred before the Cigliano eruption, between 5.25 and 4.95 ka (Smith et al., 2011; Table 1). A similar change in depositional environment from marine sediments to continental pyroclastic deposits was also detected along the easternmost sector of La Starza and in the Bagnoli and Agnano plains (Di Vito et al., 1999). The interval h1 (Fig. 9B) is characterized by a prevailing continental condition with periods of eruptive quiescence marked by the formation of paleosols. However, a layer of beach sediments (Pozzuoli unit), intercalated between Agnano Monte

Spina and Averno-Solfatara deposits, has been found along La Starza cliff. The paleontological analysis performed on sample STZA12 shows those sediments are barren, whereas similar analyses previously made on the same sediments highlighted the presence of in-situ spicules of siliceous sponges (Isaia et al., 2009) and very rare carbonate elements of organic origin that, although heavily corroded, can be attributed to bryozoans and echinoderms. Coarse sandy sediments with the same stratigraphic position and with assemblages suggesting a plausible continental/foreshore paleoenvironment (interval h2; Fig. 9B) are found in the central sector of the caldera (see Isaia et al., 2009). Both La Starza cliff and tunnel excavation successions show upward continental settings (interval h3) marked by the deposition of pyroclastic deposits of Solfatara and Averno (Pistolesi et al., 2016), Astroni (Isaia et al., 2004) and Monte Nuovo eruptions. Fossa Lupara deposit is exposed only at the Tunnel excavation entrance. The uppermost part of the reconstructed sequence, previously described as two subaerial intervals containing different volcanic units (Cinque et al., 1985; Giudicepietro, 1993), here is presented separating the different volcanic units as defined in more recent studies (e.g., Di Vito et al., 1999; and Isaia et al., 2009) and using the modelled calibrated age of Smith et al. (2011).

6. Long term ground movement

The analyzed sedimentary succession shows a sequence of depositional events outlining the interplay between inflation and deflation episodes of the caldera floor and sea level rise over the last 15 kyr. In order to compare the estimated ground vertical displacements with the sea level change in this period, we used the curve of Lambeck et al. (2011) for this part of the Italian coast (Table S4). Fig. 10A reports the paleoelevation of the well-dated deposits (points from 1 to 9). La Starza succession includes deposits 1, 2, 3, 6 and 7 whose age derive from literature (Table 1), whereas the 4, 5, 8 and 9 ages are inferred from the stratigraphic position (Fig. 9). Paleoelevation related to recent vertical deformation have been obtained from the Serapis Temple (Dvorak and Mastrolorenzo, 1991; Mohrange et al., 1999; Bellucci et al., 2006). We assumed that the Gauro Tuff deposit was emplaced in continental environments close to the shoreline, and this dated eruption represents the starting point of our kinematic reconstruction (Fig. 10A). However, no paleodepth information is available in the interval between Gauro and Pomici Principali (PP) eruptions and for the Epoch III (E3), where the most of sediments were deposited in the continental environment, except for the lower and the middle parts where in both cases the sediments were deposited close the shoreline. In the period including the Epoch I (E1) and Epoch II (E2), the La Starza sedimentation was always in marine-transitional environments (Fig. 10A), suggesting a possible balancing between the sea level rise and the ground movement. Following the emersion episode, the sedimentary structures and fossil content of sediments indicate a long period of subsidence in marine conditions starting from ca. 8.59 ka (point 6 in the Fig. 10A) up to 5.86 ka (point 7 in the Fig. 10A), when was reached the max paleodepth at about 60/80 m b.s.l. with a rate of 2.2/2.9 cm/y. The upper part of this episode also recorded an interval of alternating uplift and subsidence pulses preceding a major uplift, larger than 100 m, occurred before the beginning of the Epoch III activity. This value corresponds to the vertical displacement reached by the point 7 (Fig. 10B), however, the displacement may have reached higher values because the deposition of the volcanic rocks was in continental conditions (in this part of the CF) and there are not features to constraint the amount of uplift. During the Epoch III, an about 2.5 km^3 of magma were erupted from 28 vents (Fig. 10C) mainly located in the central-eastern sector of the caldera (Bevilacqua et al., 2016). We can only hypothesize that during the Epoch III there was mainly uplift alternated with rapid subsidence, with the interposition of the deposition of the Pozzuoli unit (point 9 in the Fig. 10A). Periods of eruptive activity of the epochs E1 (15–10.6 ka), E2 (9.6–9.1 ka) and E3 (5.5–3.8 ka) appear coupled with prevalent uplift and possible minor deflating episodes. On the contrary, the whole caldera floor subsidence occurred during quiescent periods, from 8.59 to 5.86 ka, and generally after 3.8 ka and before the Monte Nuovo eruption, as shown by borehole data of the Bagnoli and Agnano plains (e.g., Di Vito et al., 1999). The prevalent subsidence since the Roman period is also attested by submerged ruins just foreshore of La Starza ranging up to 10 m b.s.l. The historical Monte Nuovo eruption occurred at 1538 CE produced ground oscillation of about 15 m (Fig. 10A) recorded on three marble columns of the ancient Roman market in Pozzuoli, known as Serapis Temple (e.g. Parascandola, 1947; Dvorak and Mastrolorenzo, 1991; Bellucci et al., 2006; Guidoboni and Ciuccarelli, 2011; Todesco et al., 2014) and in other coastal sites of the caldera (Di Vito et al., 2016). Signs of ground movements have also been recognized at the exit of the tunnel excavation (STZD, Fig. 9D) showing the Monte Nuovo deposits covering humified marine sediments above roman ruins, at about 7 m of elevation. Elevation changes recorded in Campi Flegrei since the first leveling survey conducted in 1905–1907 CE account for early subsidence and two rapid uplift stages (1969–1972 CE and 1981–1984 CE) leading to a cumulative uplift larger than 3 m. The net vertical ground movement (Fig. 10B) was estimated as the difference between paleo– and present–elevation of the key–points in the La Starza record (Fig. 10A).

The long term ground movement reconstruction, here presented, shows a striking similarity in terms of unrest phenomena predating the Monte Nuovo eruption, which has been preceded by ground uplift episodes reaching a maximum displacement of about 15 m in the central sector of the caldera. This uplifted sector is very close inland to the La Starza area and also corresponds to the area of maximum deformation recorded since 1905/1907 CE and during the ongoing unrest crisis, which leads to a cumulative increase in the height of 4 m. The similarity in the deformation pattern within the central sector of the caldera during the time, suggests a possible common magmatic source for the different ground movements episodes, despite the entity of the ground deformation.

The recurrence of plurimetric ground uplift in the central sector of the caldera seems to be a magmatic signal likely associated with the eruptive activity. An eccentric and more concentrated ground deformation respect to the main dome growth at the caldera center could suggest the possible dike intrusion and new vent opening, as for the Monte Nuovo eruption (e.g., Di Vito et al., 2016).

Campi Flegrei caldera is a case type volcano for both long and short term ground deformation reconstruction. The results obtained by the multidisciplinary data analyzed in this paper could also suggest applying the same methods and hypothesis for caldera systems worldwide affected by hazardous phenomena as doming and unrest, especially for long term quiescent volcanoes.

7. Concluding remarks

New stratigraphic and paleoecological studies of the key-successions exposed along the La Starza marine cliff and along an ideally continuous succession excavated for a tunnel of about 1 km in length have been presented. Original field and borehole data in addition to sedimentological and paleontological analyses of the studied deposits, show that marine and subaerial conditions alternated through time. Fossil remains and sedimentary structures show that marine sediments were deposited in different environments, mainly in relation to an appreciable sea level rise but also following ground movements. The reconstruction of the paleoenvi-

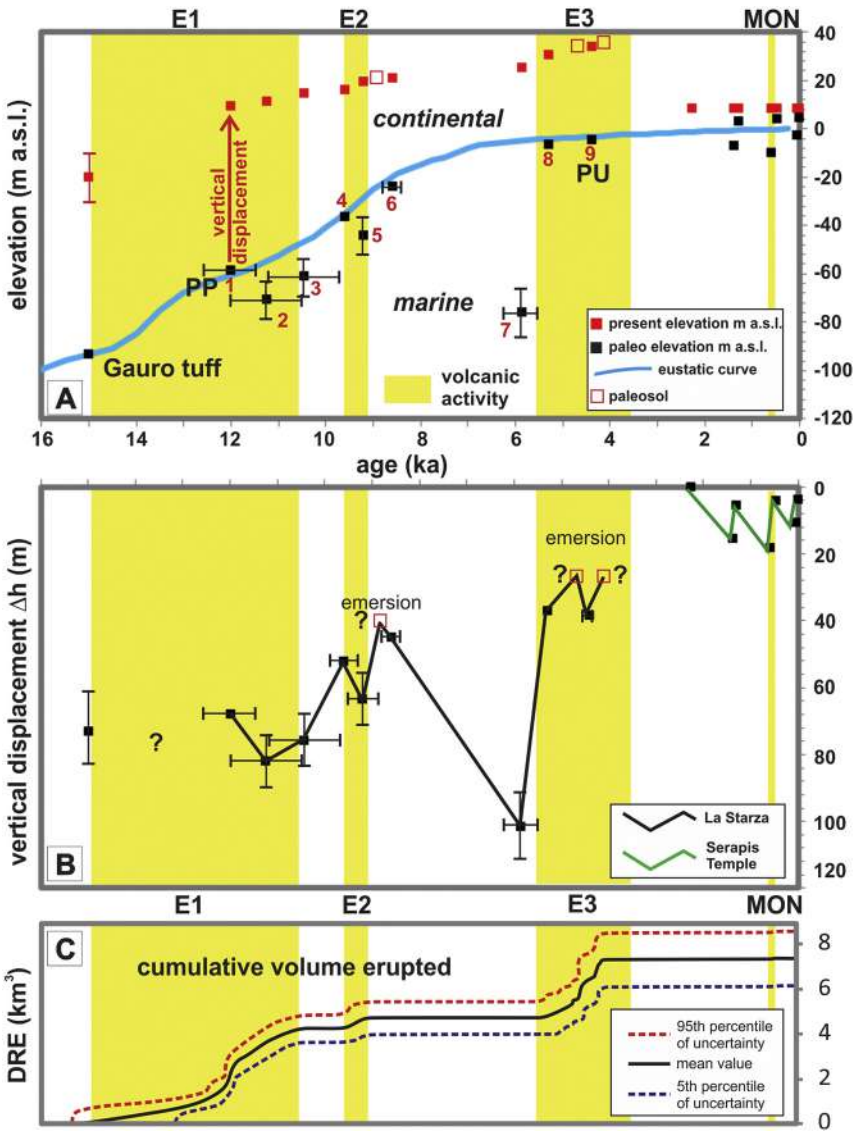

Fig. 10. A) Paleodepth and present elevation a.s.l. of the deposits exposed in the La Starza cliff and Serapis Temple (Del Gaudio et al., 2010). The diagram shows also the eustatic curve (Lambeck et al., 2011). B) Vertical displacement in the last 15 kyr. C) Cumulative volume erupted curve (from Bevilacqua et al., 2017, modified). PP: Pomici Principali; PU: Pozzuoli unit; MON: Monte Nuovo; E1-E2-E3: Epochs.

ronment evolution of the area, in relation with caldera volcanism, provides new constraint to interpret and evaluate the long- term history of the ground movements of the central sector of the Campi Flegrei caldera during the last 15 kyr.

Two main episodes of uplift were reconstructed related to volcanic activity bounding a subsiding period characterized by relative quiescence from 8.59 to 5.86 ka when a max assessed paleodepth of 60/80 m b.s.l. was reached. A brief period of ground-level oscillation preceded the start of a rapid ground uplift of 100 m coupled to the 5.5–3.5 ka volcanic activity producing a total of 2.5 km^3 of erupted magma. Oscillations in the vertical movement have been recorded by the La Starza sediments as well as detected both before Monte Nuovo eruption and more recently up to now. Despite the entity and the average rate of the different uplift episodes, the pattern of the ground deformation is similar through the time. The history of the uplift-subsidence of the central sector of the CF caldera in the last 15 kyr, previously poorly constrained, becomes now well-documented for the first time. Estimating the long-term ground movements suggests a coupling of long periods of uplift, eruptive activity, and possible deep magma movements. This long-term record also provides information on caldera unrest, dynamics, and resurgence, which are crucial issues, especially in an active volcanic area.

Supplementary data to this article can be found online at https://doi.org/10.1016/j.jvolgeores.2019.07.012.

Acknowledgments

First of all, we thank the SABESA S.p.A. staff in charge of the tunnel excavation for the opportunity to make stratigraphy logs and collect rock samples. Special thanks to the Ing Marco Porta and his closest collaborators for the great hospitality and collaboration. Victoria C. Smith (Oxford University, UK) kindly acknowledged for the ^{14}C AMS age calibration. Finally, we thank Giuseppe Brandi and Mario Dolce (INGV-Osservatorio Vesuviano) for the topographic measurements and Valeria Zamparelli for the photograph of the "mercato ortofrutticolo" outcrop.

We want to dedicate this paper to the memory of Ing Livio Cosenza, whose passion for the Campi Flegrei history and geology has contributed to the realization of this work.

References

Aiello, G., Barra, D., 2010. Crustacea, Ostracoda. Biol. Mar. Mediterr. 17 (Suppl. 1), 401–419.

Aiello, G., Barra, D., De Pippo, T., Donadio, C., 2012. Pleistocene Foraminiferida and Ostracoda from the Island of Procida (Bay of Naples, Italy). Boll Soc Paleont It 51 (1), 49–62.

Aiello, G., Barra, D., Parisi, R., Isaia, R., Marturano, A., 2018. Holocene benthic foraminiferal and ostracod assemblages in a paleo-hydrothermal vent system of Campi Flegrei (Campania, South Italy). Palaeontol. Electron. 21.3 (41A), 1–71.

Albert, P.G., Giaccio, B., Isaia, R., Costa, A., Niespolo, E.M., Nomade, S., 2019. Evidence for a large-magnitude eruption from Campi Flegrei caldera (Italy) at 29 ka. Geology 47, 595–599.

Amore, O., Barra, D., Ciampo, G., Ruggiero Taddei, E., Russo, G.F., Sgarrella, F., 1988. Il terrazzo della Starza: associazioni fossili e batimetria. Mem Soc Geol It 41, 969–981.

Amoruso, A., Crescentini, L., Sabbetta, I., 2014. Paired deformation sources of the Campi Flegrei caldera (Italy) required by recent (1980–2010) deformation history. Journal of Geophysical Research-Solid Earth 119, 858–879.

Balassone, G., Aiello, G., Barra, D., Cappelletti, De Bonis, A., Donadio, C., Guida, M., Melluso, L., Morra, Parisi, R., Pennetta, M., Siciliano, A., 2016. Effects of anthropogenic activities in a Mediterranean coastland: the case study of the Falerno-Domitio littoral in Campania, Tyrrhenian Sea (southern Italy). Marine Pollution Bullettin 112, 271–290.

Barbeito-Gonzalez, P.J., 1971. Ostracoden des Kustenbereiches von Naxos (Griechenland) und ihre Lebensbereiche. Mitt. Ham-burg. Zool. Mus. Inst., Bd. 67, 255–326.

Barra, D., Bonaduce, G., Ciarcia, S., 1998. Evidence of brackish lagoons in the Irpinia Southern Italy Pliocene. Boll. Soc. Paleontol. Ital. 37, 89–98.

Bellucci, F., Woo, J., Kilburn, C.R.J., Rolandi, G., 2006. Ground deformation at Campi Flegrei, Italy: implications for hazard assessment. In: Troise, C., De Natale, G., Kilburn, C.R.J. (Eds.), Mechanisms of Activity and Unrest at Large Calderas. Spec Pub Geol Soc, vol. 269. GSL, London, pp. 141–158.

Bevilacqua, A., Flandoli, F., Neri, A., Isaia, R., Vitale, S., 2016. Temporal models for the episodic volcanism of Campi Flegrei caldera (Italy) with uncertainty quantification. J. Geophys. Res. Solid Earth 121, 7821–7845.

Bevilacqua, A., Isaia, R., Neri, A., Vitale, S., Aspinall, W.P., Bisson, M., Flandoli, F., Baxter, P.J., Bertagnini, A., Esposti Ongaro, T., Iannuzzi, E., Pistolesi, M., Rosi, M., 2015. Quantifying volcanic hazard at Campi Flegrei caldera (Italy) with uncertainty assessment: I. Vent opening maps. Journal of Geophysical Research-Solid Earth 120, 2309–2329.

Bevilacqua, A., Flandoli, F., Neri, A., Isaia, R., Vitale, S., 2017. Temporal models for the episodic volcanism of Campi Flegrei caldera (Italy) with uncertainty quantification. Journal of Geophysical Research-Solid Earth 121 (11), 17821–17845.

Blair, T.C., McPherson, J.G., 1999. Grain-size and textural classification of coarse sedimentary particles. J. Sediment. Res. 69 (1), 6–19.

Bonaduce, G., Ciampo, G., Masoli, M., 1976. Distribution of Ostracoda in the Adriatic Sea. Pub Stazione Zool Napoli 40 (supp.1), 1–304.

Breman, E., 1976. The Distribution of Ostracodes in the Bottom Sediments of the Adriatic Sea. Academisch Proefschrift, Vrije Universiteitte, Amsterdam (165 pp).

Carobene, L., Brambati, A., 1975. Metodo per l'analisi morfologica quantitativa delle spiagge. Boll Soc Geol It 94, 479–493.

Chiodini, G., Paonite, A., Aiuppa, A., Costa, A., Caliro, S., De Martino, P., Acocella, V., Vandemeulebrouck, J., 2016. Magmas near the critical degassing pressure drive volcanic unrest towards a critical state. Nat. Commun. 7.

Ciarcia, S., Vitale, S., 2013. Sedimentology, stratigraphy and tectonics of evolving wedge-top depozone: Ariano Basin, southern Apennines, Italy. Sediment. Geol. 290, 27–46.

Cinque, A., Rolandi, G., Zamparelli, V., 1985. L'estensione dei depositi marini Olocenici nei Campi Flegrei in relazione alla vulcano-tettonica. Boll Soc Geol It 104, 327–348.

Clifton, H.E., 1981. Progradational sequences in Miocene shoreline deposits, southeastern Caliente Range, California. J. Sediment. Petrol. 51, 165–184.

Costa, A., Folch, A., Macedonio, G., Giaccio, B., Isaia, R., Smith, V., 2012. Quantifying volcanic ash dispersal and impact of the Campanian Ignimbrite super-eruption. Geophys. Res. Lett. 39, L10310.

D'Amico, C., Aiello, G., Barra, D., Bracone, V., Di Bella, L., Esu, D., Frezza, V., Rosskopf, C.M., 2013. Late Quaternary foraminiferal, molluscan and ostracod assemblages from a core succession in the Trigno River mouth area (Central Adriatic Sea, Italy). Boll Soc Paleont It 52 (3), 197–205.

D'Auria, L., Giudicepietro, F., Aquino, I., Borriello, G., Del Gaudio, C., Lo Bascio, D., Martini, M., Ricciardi, G.P., Ricciolino, P., Ricco, C., 2011. Repeated fluid-transfer episodes as a mechanism for the recent dynamics of Campi Flegrei caldera (1989-2010). Journal of Geophysical Research: Solid Earth 116, B04313.

D'Auria, L., Pepe, S., Castaldo, R., Giudicepietro, F., Macedonio, G., Ricciolino, P., Tizzani, P., Casu, F., Lanari, R., Manzo, M., Martini, M., Sansosti, E., Zinno, I., 2015. Magma injection beneath the urban area of Naples: a new mechanism for the 2012-2013 volcanic unrest at Campi Flegrei caldera. Sci. Rep. 5.

de Vita, S., Orsi, G., Civetta, L., Carandente, A., D'Antonio, M., Deino, A., di Cesare, T., Di Vito, M., Fisher, R.V., Isaia, R., Marotta, E., Necco, A., Ort, M.H., Pappalardo, L., Piochi, M., Southon, J., 1999. The Agnano-Monte Spina eruption (4100 years B.P.) in the restless Campi Flegrei caldera. J. Volcanol. Geotherm. Res. 91, 269–301.

Debenay, J.P., 2012. A Guide to 1,000 Foraminifera from Southwestern Pacific: New Caledonia. IRD Éditions, Institut de recherche pour le développement, Marseille, Publivations Scientifiques du Muséum, Muséum national d'Histoire naturelle, Paris (385 pp).

Deino, A.L., Orsi, G., Piochi, M., de Vita, S., 2004. The age of the Neapolitan Yellow Tuff caldera-forming eruption (Campi Flegrei caldera – Italy) assessed by 40Ar/39Ar dating method. J Volcanol Geoth Res 133, 157–170.

Del Gaudio, C., Aquino, I., Ricciardi, G.P., Ricco, C., Scandone, R., 2010. Unrest episodes at Campi Flegrei: a reconstruction of vertical ground movements during 1905–2009. J. Volcanol. Geotherm. Res. 185, 48–56.

Di Renzo, V., Arienzo, I., Civetta, L., D'Antonio, M., Tonarini, S., Di Vito, M.A., Orsi, G., 2011. The magmatic feeding system of the Campi Flegrei caldera: architecture and temporal evolution. Chem. Geol. 281, 227–241.

Di Vito, M.A., Isaia, R., Orsi, G., Southon, J., de Vita, S., D'Antonio, M., Pappalardo, L., Piochi, M., 1999. Volcanism and deformation in the past 12 ka at the Campi Flegrei caldera (Italy). J. Volcanol. Geotherm. Res. 91, 221–246.

Di Vito, M.A., Acocella, V., Aiello, G., Barra, D., Battaglia, M., Carandente, A., Del Gaudio, C., de Vita, S., Ricciardi, G.P., Ricco, C., Scandone, R., Terrasi, F., 2016. Magma transfer at Campi Flegrei caldera (Italy) before the 1538 AD eruption. Sci. Rep. 6, 32245.

Dvorak, J.J., Mastrolorenzo, G., 1991. The mechanisms of recent vertical crustal movements in Campi Flegrei caldera, southern Italy. Geol. Soc. Am. Spec. Pap. 263, 1–47.

Giaccio, B., Isaia, R., Fedele, F., Di Canzio, E., Hoffecker, J., Ronchitelli, A., Sinitsyn, A., Anikovich, M., Lisitsyn, S., Popov, V., 2008. The Campanian Ignimbrite and Codola tephra layers: two temporal/stratigraphic markers for the Early Upper Palaeolithic in southern Italy and eastern Europe. J Volcanol Geoth Res 177, 208–226.

Giudicepietro, F., Ph.D. thesis 1993. La dinamica recente dell'area vulcanica flegrea. University of Naples (179p).

Guidoboni, E., Ciuccarelli, C., 2011. The Campi Flegrei caldera: historical revision and new data on seismic crises, bradyseisms, the Monte Nuovo eruption and ensuing earthquakes (twelfth century 1582 AD). Bull. Volcanol. 73, 655–677.

Hart, B.S., Plint, A.G., 1995. Gravelly shoreface and beachface deposits. In: Plint, A.G. (Ed.), Sedimentary Facies Analysis. Int Ass Sed, Spec Publ, vol. 22, pp. 75–99.

Isaia, R., D'Antonio, M., Dell'Erba, F., Di Vito, M., Orsi, G., 2004. The Astroni volcano: the only example of close eruptions within the same vent area in the recent history of the Campi Flegrei caldera (Italy). J. Volcanol. Geotherm. Res. 133, 71–192.

Isaia, R., Marianelli, P., Sbrana, A., 2009. Caldera unrest prior to intense volcanism in Campi Flegrei (Italy) at 4.0 ka B.P.: implications for caldera dynamics and future eruptive scenarios. Geophys. Res. Lett. 36, L21303.

Isaia, R., Vitale, S., Di Giuseppe, M.G., Iannuzzi, E., Tramparulo, F.D.A., Troiano, A., 2015. Stratigraphy, structure and volcano-tectonic evolution of Solfatara maar-diatreme (Campi Flegrei, Italy). Geol. Soc. Am. Bull. 127, 1485–1504.

Kennedy, B., Wilcox, J., Stix, J., 2012. Caldera resurgence during magma replenishment and rejuvenation at Valles and lake City calderas. Bull. Volcanol. 74, 1833–1847.

Lambeck, K., Antonioli, F., Anzidei, M., Ferranti, L., Leoni, G., Scicchitano, G., Silenzi, S., 2011. Sea level change along the Italian coast during the Holocene and projections for the future. Quat. Int. 232, 250–257.

Macedonio, G., Giudicepietro, F., D'Auria, L., Martini, M., 2014. Sill intrusion as a source mechanism of unrest at volcanic calderas. J. Geophys. Res. 119, 3986–4000.

Mangoni, O., Aiello, G., Balbi, S., Barra, D., Bolinesi, F., Donadio, C., Ferrara, L., Guida, M., Parisi, R., Pennetta, M., Trifuoggi, M., Arienzo, M., 2016. A multidisciplinary approach forthe characterization of the coastal marine ecosystems of Monte Di Procida (Campania, Italy). Marine Pollution Bull 112, 443–451.

Marturano, A., Isaia, R., Aiello, G., Barra, D., 2018. Complex dome growth at Campi Flegrei Caldera (Italy) in the last 15ka. J. Geophys. Res. Solid Earth 123 (9), 8180–8197.

Massari, F., Parea, G.C., 1988. Progradational gravel beach sequences in a moderate- to high-energy, microtidal marine environment. Sedimentology 35, 881–913.

McCubbin, D.G., 1982. Barrier island and strand plain facies. In: Scholle, P.A., Spearing, D. (Eds.), Sandstone Depositional Environments. AAPG, pp. 247–279.

Milker, Y., Schmiedl, G., 2012. A taxonomic guide to modern benthic shelf foraminifera of the western Mediterranean Sea. Palaeontol. Electron. 15 (2.16A) (134 p).

Mohrange, C., Bourcier, M., Laborel, J., Giallanella, C., Gorain, J.P., Crimaco, L., Vecchi, L., 1999. New data on historical relative sea level movements in Pozzuoli, phlaegrean fields, Southern Italy. Phys. Chem. Earth Solid Earth Geod. 24, 349–354.

Müller, G.W.,1894. Die Ostracoden des Golfes von Neapel und der angrenzendenMeeres-Abschnitte. In: Fauna und Flora des Golfes von Neapel und der angrenzenden Meeres-Abschnitte. Herausgegeben von der Zoologischen Station zu Neapel, pp. 1–404, 1-8. (40 pls).

Neri, A., Bevilacqua, A., Esposti Ongaro, T., Isaia, R., Aspinall, W.P., Bisson, M., Flandoli, F., Baxter, P.J., Bertagnini, A., Iannuzzi, E., Pistolesi, M., Rosi, M., Vitale, S., 2015. Quantifying Volcanic Hazard at Campi Flegrei Caldera (Italy) With Uncertainty Assessment: II.

Orsi, G., D'Antonio, M., de Vita, S., Gallo, G., 1992. The Neapolitan Yellow Tuff, a large-magnitude trachytic phreatoplinian eruption: eruptive dynamics, magma withdrawal and caldera collapse. J. Volcanol. Geotherm. Res. 53, 275–287.

Orsi, G., Di Vito, M., de Vita, S., 1996. The restless, resurgent Campi Flegrei Nested Caldera (Italy): constraints on its evolution and configuration. J Volcanol Geoth Res 74, 179–214.

Parascandola, A., 1947. I fenomeni bradisismici del Serapeo di Pozzuoli. Stab Tipogr Genovese Napoli (156 pp).

Passariello, I., Talamo, P., D'Onofrio, A., Barta, P., Lubritto, C., Terrasi, F., 2010. Contribution of the Radiocarbon dating to the chronology of Eneolithic in Campania (Italy). Geochronometria 35, 25–33.

Pistolesi, M., Isaia, R., Marianelli, P., Bertagnini, A., Fourmentraux, C., Albert, P.G., Tomlinson, E.L., Menzies, M.A., Rosi, M., Sbrana, A., 2016. Simultaneous eruptions from multiple vents at Campi Flegrei (Italy) highlight new eruption processes at calderas. Geology 44, 487–490.

Reimer, P.J., Bard, E., Bayliss, A., Beck, J.W., Blackwell, P.G., Bronk Ramsey, C., Buck, C.E., Cheng, H., Edwards, R.L., Friedrich, M., Grootes, P.M., Guilderson, T.P., Haflidason, H., Hajdas, I., Hatté, C., Heaton, T.J., Hoffmann, D.L., Hogg, A.G., Hughen, K.A., Felix Kaiser, K., Kromer, B., Manning, S.W., Niu, M., Reimer, R.W., Richards, D.A., Marian Scott, E., Southon, J.R., Staff, R.A., Turney, C.S.M., van der Plicht, J., 2013. INTCAL13 and MARINE13 Radiocarbon Age Calibration Curves 0-50,000 years CAL BP. Radiocarbon 55, 1869–1887.

Rosi, M., Sbrana, A., 1987. The Phlegraeanfields: CNR Quad. de "La ricerca Scientifica". , 1–175.

Scarpati, C., Cole, P., Perrotta, A., 1993. The Neapolitan Yellow Tuff - a large volume multiphase eruption from Campi Flegrei, southern Italy. Bull. Volcanol. 55, 343–356.

Schwartz, K.S., 1982. Bedform and stratification characteristic of some modern small-scale washover sand bodies. Sedimentology 29, 835–849.

Sen Gupta, B.K., Lobegeier, M.K., Smith, L.E.,2009. Foraminiferal Communities of Bathyal Hydrocarbon Seeps, Northern Gulf of Mexico: A Taxonomic, Ecologic, and Geologic Study. In: OCS Study MMS 2009-013. U.S. Dept. of the Interior, Minerals Management Service, Gulf of Mexico OCS Region, New Orleans, LA (385 pp).

Smith, V.C., Isaia, R., Pearce, N.J.C., 2011. Tephrostratigraphy and glass compositions of post-15 kyr Campi Flegrei eruptions: implications for eruption history and chronostratigraphic markers. QuatSci Rev 30, 3638–3660.

Swift, D.J.P., Phillips, S., Thorne, J.A., 2009. Sedimentation on continental margins, VI: lithofacies and depositional systems. In: Swift, D.J.P., Oertel, G.F., Tillman, R.W., Thorne, J.A. (Eds.), Sand and Sandstone Bodies - Geometry, Facies and Sequence Stratigraphy. Int Ass Sed, Spec Pub, vol. 14, pp. 89–152.

Tizzani, P., Battaglia, M., Zeni, G., Atzori, S., Berardino, P., Lanari, R., 2009. Uplift and magma intrusion at Long Valley caldera from InSAR and gravity measurements. Geology 37, 63–66.

Todesco, M., Costa, A., Comastri, A., Colleoni, F., Spada, G., Quareni, F., 2014. Vertical ground displacement at Campi Flegrei (Italy) in the fifth century: rapid subsidence driven by pore pressure drop. Geophys. Res. Lett. 41, 1471–1478.

Vitale, S., Ciarcia, S., 2018. Tectono-stratigraphic setting of the Campania region (southern Italy). Journal of Maps 14, 9–21.

Vitale, S., Isaia, R., 2014. Fractures and faults in volcanic rocks (Campi Flegrei, southern Italy): insight into volcano-tectonic processes. Int J Earth Sc 103, 801–819.

Vitale, S., Isaia, R., Ciarcia, S., Di Giuseppe, M.G., Iannuzzi, E., Prinzi, E.P., Tramparulo, F.D.A., Troiano, A., 2019. Seismically induced soft-sediment deformation phenomena during the volcano-tectonic activity of Campi Flegrei caldera (southern Italy) in the last 15 kyr. Tectonics, http://dx.doi.org/10.1029/2018TC005267.

Woo, J.Y.L., Kilburn, C.R.J., 2010. Intrusion and deformation at Campi Flegrei, southern Italy: sills, dikes, and regional extension. J. Geophys. Res. 115, B12210.